



Title	BXSB/MpJ-Yaa mouse model of systemic autoimmune disease shows increased apoptotic germ cells in stage XII of the seminiferous epithelial cycle
Author(s)	Otani, Yuki; Ichii, Osamu; Masum, Abdul; Kimura, Junpei; Nakamura, Teppei; Elewa, Yaser Hosny Ali; Kon, Yasuhiro
Citation	Cell and tissue research, 381, 203-216 <a href="https://doi.org/10.1007/s00441-020-03190-0">https://doi.org/10.1007/s00441-020-03190-0</a>
Issue Date	2020-04-04
Doc URL	<a href="http://hdl.handle.net/2115/80847">http://hdl.handle.net/2115/80847</a>
Rights	This is a post-peer-review, pre-copyedit version of an article published in Cell and tissue research. The final authenticated version is available online at: <a href="http://doi.org/10.1007/s00441-020-03190-0">http://doi.org/10.1007/s00441-020-03190-0</a>
Type	article (author version)
File Information	Cell and tissue research_381_203-216.pdf



[Instructions for use](#)

**Title Page**

**BXSB/MpJ-Yaa mouse model of systemic autoimmune disease shows increased apoptotic germ cells in stage XII of the seminiferous epithelial cycle**

Yuki Otani<sup>1</sup>, Osamu Ichii<sup>1,2</sup>, Md. Abdul Masum<sup>1</sup>, Junpei Kimura<sup>1</sup>, Teppei Nakamura<sup>1,3</sup>, Yaser Hosny Ali Elewa<sup>1,4</sup>, Yasuhiro Kon<sup>1\*</sup>

1. Laboratory of Anatomy, Department of Basic Veterinary Sciences, Faculty of Veterinary Medicine, Hokkaido University, Kita 18 Nishi 9, Kita-ku, Sapporo, Japan

2. Laboratory of Agrobiomedical Regenerative Medicine, Faculty of Agriculture, Hokkaido University, Kita 9 Nishi 9, Kita-ku, Sapporo, Japan

3. Section of Biological Safety Research, Chitose Laboratory, Japan Food Research Laboratories, 2-3, Bunkyo, Chitose, Japan

4. Department of Histology, Faculty of Veterinary Medicine, Zagazig University, Zagazig, Egypt

\*: Corresponding author (Tel: +81-11-706-5189; Email: y-kon@vetmed.hokudai.ac.jp).

**Acknowledgments and Funding Information**

This study was supported in part by JSPS KAKENHI (grant number JP18J22455). The research described in this paper was chosen for the Best Poster Presentation Award at the 6th Congress of Asian Association of Veterinary Anatomists in Malaysia (14-15 October 2017), and the Encouragement Award at the 161st Japanese Association of Veterinary Anatomists in Ibaraki (11-13 September 2018).

## Abstract

In mammals, the reproductive system and autoimmunity regulate mutual functions. Importantly, systemic autoimmune diseases are thought to cause male infertility, but the underlying pathological mechanism remains unclear. In this study, the morpho-function of the testes in BXSB/MpJ-*Yaa* mice were analyzed as a representative mouse model for systemic autoimmune diseases to investigate the effect of excessive autoimmunity on spermatogenesis. At 12 and 24 weeks of age, BXSB/MpJ-*Yaa* mice showed splenomegaly and increased levels of serum autoantibodies, whereas no controls showed similar autoimmune condition. In histological analysis, the enlarged lumen of the seminiferous tubules accompanied with scarce spermatozoa in the epididymal ducts were observed in some of the BXSB/MpJ-*Yaa* and BXSB/MpJ mice, but not in C57BL/6N mice. Histoplanimetric analysis revealed significantly increased residual bodies and apoptotic germ cells in the seminiferous tubules in BXSB/MpJ-*Yaa* testes without apparent inflammation. Notably, in stage XII of the seminiferous epithelial cycles, the apoptotic germ cell number was remarkably increased, showing a significant correlation with the indices of systemic autoimmune disease in BXSB/MpJ-*Yaa* mice. Furthermore, the Sertoli cell number was reduced at the early disease stage, which likely caused subsequent morphological changes in BXSB/MpJ-*Yaa* testes. Thus, our histological study revealed the altered morphologies of BXSB/MpJ-*Yaa* testes, which were not observed in controls, and statistical analysis suggested the effects of an autoimmune condition on this phenotype, particularly the apoptosis of meiotic germ cells. BXSB/MpJ-*Yaa* mice were shown to be an efficient model to study the relationship between systemic autoimmune disease and the local reproductive system.

**Keywords:** Systemic autoimmune disease; Male infertility; Spermatogenesis; Apoptosis; Meiosis

## LIST OF ABBREVIATIONS

48	
49	ASA: anti-sperm antibody
50	BTB: blood-testis barrier
51	BXSB: BXSB/MpJ- <i>Yaa</i> <sup>+</sup>
52	BXSB- <i>Yaa</i> : BXSB/MpJ- <i>Yaa</i>
53	CB: citrate buffer
54	DNA: deoxyribonucleic acid
55	dsDNA: double-stranded DNA
56	EAO: experimental autoimmune orchitis
57	ELISA: enzyme-linked immunosorbent assay
58	Foxp3: forkhead box P3
59	IL: interleukin
60	lpr: lymphoproliferation
61	Nos: nitric oxide synthase
62	PAS: periodic acid-Schiff
63	RNA: ribonucleic acid
64	S/B: the ratio of spleen weight to body weight
65	SE: standard error
66	SLE: systemic lupus erythematosus
67	ssDNA: single-stranded DNA
68	St.: stage of seminiferous epithelial cycle
69	tACE: testicular isoform of angiotensin-converting enzyme
70	Tgf: transforming growth factor
71	Tlr: toll-like receptor

72    Tnf: tumor necrosis factor

73    Yaa: Y-linked autoimmune acceleration

## 1. Introduction

In mammals, immunity contributes to the maintenance of reproductive function. For female reproduction, the proper activation of local immunity by resident immune cells, such as macrophages and T-cells, plays a role in the ovulation or regression of the corpus luteum in the ovaries (Komatsu et al. 2003). In contrast, testes have a unique immunological feature, known as immune privilege. Immunosuppression is essential to maintain germ cells and appropriate spermatogenesis because components of germ cells that express after immune competence is established can be recognized as autoantigens and attacked by the immune system. Notably, the tight junction, called the blood-testis barrier (BTB) and formed by adjacent Sertoli cells, partially segregates spermatogenic cells from systemic immune factors and prevents systemic immune factors from invading the adluminal compartment. In addition, anti-inflammatory factors, such as Interleukin- (IL) 10 are produced by testicular interstitial cells and resident immune cells, to maintain an immunosuppressed environment (Fijak and Meinhardt 2006).

On the other hand, sex-related factors also affect the immune system. The X chromosome encodes several immune-associated genes, and several X-linked gene mutations have been determined as causing immunodeficiency. Briefly, a mutation in the  $\gamma$ -chain subunit forming IL-2, IL-4, IL-7, IL-9, IL-15, and IL-21 receptors causes X-linked severe combined immunodeficiency. Forkhead box P3 (*Foxp3*) is also identified as a causative gene for immune dysregulation, polyendocrinopathy, enteropathy, and X-linked syndrome in humans (Fish 2008). Furthermore, sex hormones play essential roles in the activation or suppression of the immune system. As a representative, estrogen receptors expressed in immune cells activate or suppress their functions, depending on the concentration of estrogen (Kovats 2015). Androgen appears to promote IL-10 secretion from T-cells and suppresses the function of dendritic cells or macrophages (Trigunaite et al. 2015).

Due to a close functional relationship between the immune and reproductive systems, abnormality in one system is often reflected in the other. In fact, 30% of patients with premature ovarian failure also have an autoimmune disease (Goswami and Conway 2007). Anti-sperm antibodies (ASA) are frequently detected in infertile men (Garcia et al. 2007), resulting in decreased sperm concentration and motility (Cui et al. 2015). Furthermore, secondary autoimmune orchitis leading to infertility is reported in patients with systemic autoimmune diseases, such as systemic lupus erythematosus (SLE), Behçet's disease, and rheumatoid arthritis. Furthermore, ASA is present in half of the patients with SLE (Silva et al. 2014). For research purposes, experimental autoimmune orchitis (EAO) can be induced by immunization with testicular homogenate and adjuvant in mice, rats, rabbits, and guinea pigs (Naito et al. 2012). EAO, resulting in infertility, is histopathologically characterized by T-cell-dependent lymphocytic inflammation and damaged seminiferous tubules, with disruption of the BTB (Kohno et al. 1983). In these patients and model animals, the abnormality of systemic or local immune systems causes reproductive system-related phenotypes, but detailed pathogenesis is unknown.

In this study, we examined the pathological features of the male reproductive system in a male-dominant systemic autoimmune disease mouse model. The BXS<sub>B</sub> strain is derived from an intercross of C57BL/6J and SB/Le mouse (Andrews et al. 1978). It has been found that some mutants in the BXS<sub>B</sub> strain are characterized by autoantibody production, splenomegaly, and severe lupus nephritis-like features due to the excessive proliferation of autoreactive lymphocytes (Suzuka et al. 1993). These mutants carry a Y-linked autoimmune acceleration (*Yaa*) mutation, a translocation of some genes on the X chromosome telomere region to that of the Y chromosome. *Yaa* mutation has been identified as the most potent causative molecule to mediate autoimmune disorder in these mutants, designated as BXS<sub>B</sub>/MpJ-*Yaa* (BXS<sub>B</sub>-*Yaa*,

Murphy and Roths 1979). In addition, previous studies revealed the BXSB genome is also suspected of forming autoimmune disease-prone phenotypes, as aged female BXSB/MpJ (BXSB, without *Yaa* mutation) mouse manifested autoantibody production and glomerulonephritis (Boehm et al. 1998; Kimura et al. 2014).

Here we showed the histopathological abnormalities of the BXSB-*Yaa* testis, characterized by increases of residual bodies and apoptotic germ cells in stage XII of the seminiferous epithelial cycle, which were closely correlated with systemic autoimmune abnormalities. We further demonstrated the change of Sertoli cell number was associated with the progression of an autoimmune condition, which likely caused subsequent morphological changes in BXSB-*Yaa* testes. Our results provide a novel insight into the pathogenesis of reproductive dysfunction associated with systemic autoimmune abnormality.



## **2. Materials and methods**

### ***2.1. Animals and sample preparation***

Male C57BL/6N, BXSB, and BXSB-*Yaa* mice were purchased from Japan SLC, Inc. (Hamamatsu, Shizuoka, Japan). Twelve- and 24-week-old mice were used in all experiments. Mice were maintained according to The Guide for the Care and Use of Laboratory Animals of Hokkaido University, and all animal experiments were approved by the Institutional Animal Care and Use Committee, Hokkaido University and the Faculty of Veterinary Medicine, Hokkaido University (approval No. 15-0079, 16-0124; approved by the Association for Assessment and Accreditation of Laboratory Animal Care International). Body weights were measured, followed by the collection of blood samples by cutting the carotid artery under deep anesthesia. After euthanasia by cervical dislocation, the testes, epididymides, and spleen were collected. The weights of the spleen and testes were measured, and the ratio to body weight was compared in each group, respectively.

### ***2.2. Evaluation of serum autoantibodies***

To evaluate the systemic autoimmune conditions, serum anti-double-stranded DNA (dsDNA) antibody levels were measured using the Mouse Anti-dsDNA ELISA KIT (Shibayagi, Gunma, Japan) according to the manufacturer's instructions.

### ***2.3. Histological analysis***

Collected organs were fixed in 4% paraformaldehyde (for immunohistochemistry) or Bouin's fluid overnight, were embedded in paraffin, then cut into sections (2-3  $\mu$ m thick). Deparaffinized sections were stained with periodic acid-Schiff (PAS) to determine the stages of the seminiferous epithelial cycle (St.).

The immunodetection of cell markers for T-cells (CD3), B-cells (B220), macrophages (Iba1), and apoptotic cells [single-stranded DNA (ssDNA)] was performed as follows: for antigen retrieval, sections were incubated in buffered citrate (pH 6.0) for 15 min at 110°C. The samples were soaked in methanol containing 0.3% H<sub>2</sub>O<sub>2</sub> to block internal peroxidase activity. After blocked in 10% normal goat serum (SABPO(R) Kit, Nichirei, Tokyo, Japan), or 10% normal donkey serum (Sigma-Aldrich, Missouri, USA) for 1 hour at room temperature, sections were incubated with primary antibodies listed in Table 1 at 4°C overnight. After washing 3 times in Phosphate buffered saline, sections were incubated with biotin-conjugated goat anti-rabbit IgG antibody (SABPO(R) Kit, Nichirei), or donkey anti-rat IgG antibody (Sant Cruz, California, USA) for 30 min at room temperature, washed again, and incubated with streptavidin-biotin complex (SABPO(R) Kit, Nichirei) for 30 min. The sections were then incubated with 3, 3'-diaminobenzidine tetrahydrochloride-H<sub>2</sub>O<sub>2</sub> solution. Finally, the sections were counterstained with PAS-hematoxylin staining. When the St. in more than 80% of the seminiferous tubules could not be classified due to morphological abnormalities, these testis specimens were excluded from the histoplanimetric analysis.

#### **2.4. Histoplanimetry**

Histoplanimetric analysis for the testes was performed as follows:

- (a) *The number and area of the seminiferous tubules:* Histological sections were converted into digital images by scanning with NanoZoomer 2.0-RS and observed with NDP.view2 program (Hamamatsu Photonics K.K., Hamamatsu, Shizuoka, Japan). In a PAS-stained section, each St. of the seminiferous tubules was classified based on the morphological characteristics of the seminiferous tubules (Meistrich and Hess 2013). The number and area of the seminiferous tubules were quantified at each St. with

NDP.view2. These values were also used in the following measurements.

(b) *The number of residual bodies in seminiferous tubules:* Digitally imaged sections with NanoZoomer 2.0-RS were used. The numbers of residual bodies with more than 10  $\mu\text{m}$  of the minor axis were counted at each classified St. according to analysis (a).

(c) *The number of ssDNA-positive cells in seminiferous tubules:* Sections digitally imaged with NanoZoomer 2.0-RS were used. The number of ssDNA-positive cells in a seminiferous tubule was counted at each classified St. according to analysis (a).

(d) *The number of Sertoli cells in seminiferous tubules:* Sections digitally imaged with NanoZoomer 2.0-RS were used. The number of Sertoli cells in a seminiferous tubule was counted at each classified St. according to analysis (a). The Sertoli cell was histologically identified by its basal localization and morphology with apparent nucleoli.

For quantification, the total numbers of residual bodies, ssDNA-positive cells, and Sertoli cells were divided by the total area of the seminiferous tubules at each St., in a section.

## **2.5. Reverse transcription and quantitative PCR (qPCR)**

Total RNA was isolated from the testes using the TRIzol Reagent (Life Technologies, California, USA), following the manufacturer's protocol. cDNA was synthesized from total RNA by reverse transcription (RT) using the ReverTra Ace qPCR RT Master Mix with gDNA Remover (TOYOBO, Osaka, Japan). Gene expression levels were examined by using synthesized cDNA, THUNDERBIRD SYBR qPCR Mix (TOYOBO, Osaka, Japan), and a real-time thermal cycler (CFX Maestro; BIO-RAD, California, USA), according to the manufacturer's instructions. Gene expression in the testes was normalized to the expression of actin, beta (*Actb*). The details of primers are shown in Table 2.

205

206 **2.6. Statistical analysis**

207       The results are expressed as mean  $\pm$  standard error (SE) and were analyzed using  
208 non-parametric statistical methods. Data among strains of the same age were compared using  
209 the Kruskal-Wallis test, and multiple comparisons were performed using Scheffe's method when  
210 significant differences were observed ( $P < 0.05$ ). Data between different ages in the same strain  
211 were compared using the Mann-Whitney  $U$ -test ( $P < 0.05$ ). Spearman's correlation coefficient  
212 ( $P < 0.05$ ) was used to analyze the correlation between two parameters.

### 3. Results

#### 3.1. Indices of the autoimmune condition and reproductive function of mice

Figure 1a shows the bodyweight of animals. BXSB and BXSB-*Yaa* showed significantly smaller values compared to C57BL/6N at 12 and 24 weeks of age, indicating early and late disease stages, respectively. An age-related increase was observed in C57BL/6N and BXSB-*Yaa*, but not in BXSB. The testis weight was compared as an index of male reproductive function (Borg et al. 2010). At both ages, the testis weight was significantly smallest in BXSB-*Yaa*, and BXSB also showed significantly lower values compared with C57BL/6N (Fig. 1b). No significant age-related change was observed in their testis weights. For their ratio to body weight, there was no significant strain difference at both ages, but age-related significant decreases were observed in C57BL/6N and BXSB-*Yaa* (Fig. 1c).

The ratio of spleen weight to body weight (S/B) and serum anti-dsDNA antibody levels were used as indices for the severity of systemic autoimmune disease in mice (Fig. 1d and e). BXSB-*Yaa* showed significantly higher values of both indices compared with the other two strains at both stages ( $P < 0.01$ ). In these parameters, a significant age-related increase was observed only in the S/B of BXSB-*Yaa*. Furthermore, the data of testis weight and spleen weight in all examined BXSB-*Yaa* revealed a significant negative correlation ( $\rho = -0.600$ ;  $P = 0.001$ ,  $n = 26$ ) (Fig. 1f), indicating the close relationships between male reproductive function and autoimmune disease.

#### 3.2. Histopathological features of mouse testes

Figure 2 shows representative histological images of mouse testes at 12 weeks of age. Dilated seminiferous tubules with enlarged lumens were observed in some BXSB (12 and 24 weeks of age: 40%) and BXSB-*Yaa* (12 weeks of age: 67%; 24 weeks of age: 50%), but not in

C57BL/6N at both ages (Fig. 2a-c). As correlated with the enlargement of seminiferous tubules, the epididymal ducts at the tail portion in the C57BL/6N contained numerous spermatozoa, but not in some of the mice belonging to the other two strains at 12 weeks of age (Fig. 2d-f). These findings in the seminiferous tubules and the epididymal ducts were similarly observed at 24 weeks of age. Furthermore, multinucleated cells were observed in some seminiferous tubules of BXSB-*Yaa* testis (Fig. 2g), and some of their rete testis were dilated and filled with sperm at both ages (Fig. 2h). However, these features were not observed in C57BL/6N and BXSB at any age.

On the other hand, residual bodies, globular bodies comprising redundant organelles and RNA shed from elongating spermatid during spermiation (Firlit and Davis 1965), were observed in the seminiferous tubules of all mice at both ages (Fig. 2i-k). Some residual bodies were present in the seminiferous tubules throughout St. I to XII in BXSB-*Yaa* or at most stages except for St. II to V in BXSB, whereas they were mostly found at St. VIII or IX in C57BL/6N (Supplemental figure 1). The numerical analysis confirmed that BXSB-*Yaa* showed higher numbers of residual bodies in total tubular area compared to that of C57BL/6N at both ages, and the difference was significant at 12 weeks (Fig. 2l). In each stage comparison, significant differences among strains were observed only in St. VIII (Supplemental figure 1 and Fig. 2m). Briefly, BXSB-*Yaa* and BXSB tended to show a larger number than C57BL/6N at both ages, and a significant difference was observed between BXSB-*Yaa* and C57BL/6N. A significant age-related increase was observed only in C57BL/6N at St. VIII. Furthermore, some residual bodies with atypical morphologies, characterized by larger sizes and apoptotic like bodies (Creasy et al. 2012), were still stained with tACE, a specific marker of residual bodies, as a ring shape around the body (Supplemental Figure 2a) (Tung et al. 2017). These atypical structures were observed on the luminal side of the tubules at several St.s in BXSB-*Yaa* at both ages

(Supplemental Figure 2b and Fig. 2n) (Xiao et al. 2017). As atypical residual bodies produced during failure of spermiation due to chemical injection accumulate RNA (Saito et al. 2017), larger residual bodies observed in BXSB-*Yaa* seminiferous tubules contained abundant RNA stained with pyronin (Supplemental Figure 2c). The reaction of pyronin was confirmed to be eliminated with pre-treatment of RNase (Supplemental Figure 2d).

### 3.3. Comparison of immune-related phenotypes in mouse testes

Resident immune cells in testes and cytokines released from these cells or testicular cells are essential to maintain normal testicular function, such as the proliferation and apoptosis of germ cells, and establishment of BTB (Theas 2018). First, the infiltration and distribution of immune cells were analyzed by immunohistochemistry, since infiltrated immune cells as testicular inflammation affect spermatogenesis (Fig. 3). As a result, no CD3-positive T-cells and B220-positive B-cells were found in the testes of all examined strains at both ages (Fig. 3a-f). Iba1-positive macrophages were observed in the interstitium in all examined strains (Fig. 3g-i), but their distribution and appearance frequency did not alter among strains and ages (data not shown).

The mRNA expression levels of pro-/anti-inflammatory genes (*Il1a*, *Il1b*, *Nos2*, *Il6*, *Tnf*, *Tgf*, and *Il10*) in mice testes were evaluated by qPCR. There was no significant strain- or age-related difference among the examined strains (Fig. 3j).

### 3.4. Apoptotic cells in mouse testes

Apoptotic cell death is an essential process during spermatogenesis, in particular, for the removal of abnormal germ cells and maintaining the appropriate germ cell to Sertoli cell ratio (Giampietri et al. 2005). As a pathological condition, toxic, chemical, and genetic factors could

induce the apoptosis of germ cells (Shaha et al. 2010). Furthermore, in the testes with autoimmune orchitis, apoptotic germ cells are observed frequently, resulting in infertility (Naito et al. 2012). Immunohistochemical analysis was performed to detect apoptotic cells in the mouse testes, and Figure 4a to c show the representative images of ssDNA-positive apoptotic germ cells at 12 weeks, and they were observed in the seminiferous tubules of all strains at both ages. In numerical comparison, the mean number of ssDNA-positive germ cells in all examined areas of total tubules was highest in BXSB-*Yaa* compared with other strains at both ages (Fig. 4d). Notably, in the stage comparison, ssDNA-positive apoptotic germ cells were frequently observed in St. XII seminiferous tubules of all strains (Fig. 4e). Furthermore, significant differences among strains and ages were observed at St. XII as well as St. IV. For St. XII, BXSB-*Yaa* showed the highest values in both ages, and significances were observed with two other strains and C57BL/6N at 12 and 24 weeks of age, respectively. On the other hand, at 24 weeks, these positive cells in BXSB and BXSB-*Yaa* were significantly lower than in C57BL/6N at St. IV, and BXSB-*Yaa* showing the significant age-related decrease at this stage.

Next, the number of Sertoli cells in each stage of seminiferous tubules were evaluated to examine the effect of Sertoli cells on the number of apoptotic germ cells in the seminiferous tubules. The morphology of the Sertoli cells differed among St., and obvious strain- or age-related differences were not identified (Fig. 4f-h). In the numerical analysis, there was no strain- or significant age-related differences in the mean number of Sertoli cells in all examined areas of tubules, but BXSB-*Yaa* tended to show smaller values compared with C57BL/6N and BXSB at 12 weeks (Fig. 4i). Furthermore, at 12 weeks, BXSB-*Yaa* tended to show a smaller number of Sertoli cells at all St., and significances with BXSB were observed at St. IV, V, and IX (Fig. 4j). These decreased phenotypes of Sertoli cells were not observed in 24-week-old BXSB/MpJ-*Yaa* testes. An age-related increase was detected at St. IX in BXSB-*Yaa*.



### 3.5. Correlation between testicular phenotype and autoimmune disease indices in mice

Table 3 summarizes the statistical correlation between the examined indices for testicular phenotypes and autoimmune diseases in all examined mice or BXSB-*Yaa*. In all examined mice, the ratio of testis weight to body weight showed no significant correlation with other examined parameters. For histological phenotypes, the mean number of residual bodies in all examined areas of tubules positively correlated with the serum level of the dsDNA antibody in the groups, including 12 weeks and both ages. That of the ssDNA-positive cells in all examined areas of the tubules also positively correlated with S/B in all age groups and with the serum levels of the dsDNA antibody in the groups, including 24 weeks and both ages. In contrast, the number of Sertoli cells in all examined areas of the tubules negatively correlated with the serum levels of dsDNA antibody in the 12-week-old groups. In the analysis using BXSB-*Yaa*, testis weight to body weight significantly correlated with S/B in both age groups. The mean number of residual bodies in all examined areas of the tubules also positively correlated with S/B in the 12-week-old group. On the other hand, there was no correlation in the numbers of ssDNA-positive cells and Sertoli cells in all examined areas of the tubules.

Table 4 shows the statistical correlation of the indices of autoimmune diseases with histological phenotypes that showed significant differences in the strain comparison at each St. (Supplemental figure 1, Fig. 4e and j). In the analysis of all examined mice, the number of residual bodies in tubules at St. VIII positively correlated with the serum levels of the dsDNA antibody in the groups, including 12 weeks and both ages. As for the ssDNA-positive cells, there were positive correlations in St. XII tubules with S/B in the groups, including 24 weeks and both ages and with the serum levels of the dsDNA antibody in all age groups. That of the Sertoli cells in tubules at St. IV and V negatively correlated with S/B and the serum levels of the

dsDNA antibody in the 12-week groups. In tubules at St. IX, the Sertoli cell number positively correlated with S/B in the groups including both ages, but the coefficient was low. In the analysis using BXS<sub>B</sub>-Yaa, there was no definite correlation in residual bodies at St. VIII and Sertoli cells at St. IV and IX, although the number of Sertoli cells at St. V tubules positively correlated with S/B of 12 weeks. As for the number of ssDNA in tubules at St. IV, there was a positive correlation with S/B of 24 weeks. Furthermore, the number of positive cells in tubules at St. XII clearly showed a positive correlation with S/B and the serum levels of the dsDNA antibody in the 12-week-old groups. For other St. analysis, definite correlations were not shown (Supplemental Tables 1 and 2).

#### 4. Discussion

BXSB-*Yaa* manifested the autoimmune disease phenotypes from 12 weeks, which became more severe at 24 weeks. The testis to body weight ratio decreased with disease progression and significantly correlated with the autoimmune index and spleen size in BXSB-*Yaa*. These data suggest that *Yaa* mutation-associated autoimmune abnormality can affect the male genital function. In general, the changes in testis weights reflect its histological changes, especially those of seminiferous tubules. Briefly, germ cell apoptosis inversely correlated with testis weight in mice (Otsuka et al. 2010). Indeed BXSB-*Yaa* increased the number of apoptotic germ cells. On the other hand, BXSB-*Yaa* and BXSB, but not C57BL/6N showed wider lumens of seminiferous tubules. This reasoning may be accurate as the increased luminal diameter of the seminiferous tubules was diagnosed as a dilation with increased fluid in the seminiferous tubules, which usually increases testis weight (Creasy et al. 2012). Since significant differences in the ratios of testis to body weight were not observed between healthy controls and BXSB-*Yaa*, the fluid accumulation in the testicular tubules could make testis weight loss obscure in BXSB-*Yaa*. Notably, nearly 95% of the seminiferous tubular fluid is reabsorbed in the efferent duct, and the failure of reabsorption causes fluid back pressure into seminiferous tubules, resulting in increased luminal diameter (Hess 2002). Further, the dysfunction of cilia in the efferent duct has been reported to cause male infertility with dilated seminiferous tubules and rete testis, which likely results from the failure to propel sperms from rete testis into the epididymis (Yuan et al. 2019; Terré et al. 2019). Importantly, inflammation could disrupt the morphology and function of ciliated epithelial cells (Ullrich et al. 2009; Thomas et al. 2010). Thus, the dilated seminiferous tubules would reflect the altered function of the efferent duct epithelium related to the fluid reabsorption or flow, and the inflammatory condition by the progression of systemic autoimmune disease in BXSB-*Yaa* might affect the epithelial cell

function.

In mammal testes, 75% of germ cells die during spermatogenesis through the process of apoptosis (Giampietri et al. 2005). In this study, BXS*B-Yaa* showed the increased apoptosis of St. XII at both disease stages but a decrease in that of St. IV with aging. In a previous study, we discussed that St. IV and St. XII were important for pachytene- or metaphase-specific germ cell apoptosis as checkpoints to maintain normal spermatogenesis, and the mouse genetic factors were found to affect their numbers (Otsuka et al. 2010). Therefore, the imbalanced checkpoint system between St. IV and St. XII might be involved in the quantitative alternations of apoptotic germ cells in BXS*B-Yaa*.

Importantly, St. XII showed the highest percentage among stages in the number of apoptotic germ cells of all examined mice. As for mouse St. XII, many germ cells undergo meiotic division. During meiosis, cells undergo complicated processes, such as chromosome replication, DNA double-strand break formation, spindle fiber formation, and meiotic cell division (Subramanian and Hochwagen 2014). Each process is regulated precisely and complexly; thus, some germ cells with errors undergo apoptosis at this stage (Lue et al. 2003). Notably, similar increases of dead cells at St. XII were reported in autoimmune disease-prone MRL/MpJ and MRL/MpJ-Fas<sup>lpr/lpr</sup> mice, but not in C57BL/10, CBA/J, C3H/He, BALB/c, DBA/2, NJL, and SL mice (Kon et al. 1999). Furthermore, our histoplanimetry revealed that the apoptotic cells at St. XII increased from the early disease stage and most strongly correlated with the autoimmune disease indices among examined parameters in BXS*B-Yaa*. Therefore, these results indicate that germ cells in St. XII tubules would have high susceptibility to altered immune conditions in mice and could be recognized as cells with errors.

BXS*B-Yaa* also showed the highest values in residual body numbers, in particular at St. VIII, among strains at both ages, and significantly correlated with the autoimmune disease index

at the early disease stage. A residual body is an aggregate of discarded organelles and RNA from spermatogenic cells. Residual bodies are usually observed at St. VIII and IX, as they are phagocytosed by Sertoli cells immediately after spermiation and then migrate to the basal cytoplasm of Sertoli cells (Xiao et al. 2017). Furthermore, the abnormally large size of residual bodies containing apoptotic like bodies and their appearance in St. where residual bodies are not present normally, were sometimes observed in cases of spermiation failure, caused by chemical injection (Creasy et al. 2012). Oral administration of one single chemical substance causes the decrease of Sertoli cells and increase of residual bodies, which characterizes larger sizes and the accumulation of RNA in rats (Saito et al. 2017). From these reports, it might be possible that the change of testicular microenvironment caused by a systemic autoimmune condition in BXSB-*Yaa* directly affects the process of spermiation. Further, as the number of residual bodies at St. VIII tended to increase with aging in all examined mice, BXSB-*Yaa* would accelerate its age-related functional loss of testicular cells.

The increased number of apoptosis of meiotic cells and abnormal residual bodies in BXSB-*Yaa* strongly suggested impairment of Sertoli cell function because both structures are usually phagocytized by Sertoli cells (Creasy et al. 2012; Jiang et al. 2015). Importantly, proper clearance of apoptotic germ cells and residual bodies by Sertoli cells would be necessary to prevent an autoimmune reaction against spermatogenic cells induced by autoantigens (Wu et al. 2008). Further, Sertoli cells are highly attributed toward maintaining the immune privilege of mammalian testes, establishing BTB and immunosuppressive environments to segregate germ cells from systemic autoimmunity (Fijak and Meinhardt 2006). Conversely, the current study revealed that testicular antigens, which meiotic germ cells express, egress into interstitial space through Sertoli cells, contributing toward maintaining immune tolerance (Tung et al. 2017). Contradictory to immune privilege, systemic autoimmune diseases, such as SLE, Behçet's

disease, and rheumatoid arthritis, are diagnosed as associated diseases of autoimmune orchitis leading to male infertility (Silva et al. 2014). Although the pathogenesis remains unclear, the data for male patients with SLE suggest a dysfunction in Sertoli cells. (Suehiro et al. 2008). Our histoplanimetric results revealed that Sertoli cells at St. IV-V and IX were significantly decreased in BXSB-*Yaa* compared with BXSB at the early disease stage. Importantly, in BXSB-*Yaa*, St. V and St. IX were the stages just after the spermatogenesis checkpoint at St. IV and the frequent occurrence of residual bodies at St. VIII, respectively, suggesting the relationship between Sertoli cells and germ cell alternations. On the other hand, a significant decrease of apoptotic germ cells at St. IV was observed in BXSB-*Yaa* at the late but not the early stage. In addition, these mice showed the age-related increase of Sertoli cells at St. IX. Although the pathogenesis associating with Sertoli cells was still unclear in BXSB-*Yaa*, the negative correlation between Sertoli cell numbers at St. IV-V and autoimmune disease severity at the early stage indicated the effect of autoimmune abnormalities on Sertoli cells. Taken together, further studies focusing on the direct effects of autoimmunity to germ cells as found in increased apoptosis at St. XII and the indirect effects via Sertoli cell injuries at the other stages would be beneficial.

From the genetic perspective, X-linked genes contribute to male reproductive function including meiosis (Yang et al. 2008; Zheng et al. 2010). BXSB-*Yaa* possesses excessive X-linked genetic factors, known as the genes on the *Yaa* locus (Murphy and Roths 1979), which is considered to be responsible for systemic autoimmune disease. Among the genes on the *Yaa* locus, Toll-like receptor 7 (*Tlr7*) and *Tlr8* are considered important for the development of autoimmune disease condition (Pisitkun et al. 2006). Tlr is a pattern-recognition receptor expressed on the cell or endosome membrane that plays a role in innate immunity. Notably, the expression of *Tlr* members, including *Tlr7*, in mouse testis has been identified, and the roles of

the *Tlr* family in spermatogenesis have been discussed in a previous study (Wu et al. 2008). Briefly, an *in vitro* study revealed that Tlr3 activation by polyinosinic-polycytidylic acid, induced apoptosis of spermatogonia (Hu et al. 2015). In addition, a study using *Tlr2*- and *Tlr4*-deficient mice showed that *Tlr2* and *Tlr4* contribute to the formation of autoimmune orchitis (Liu et al. 2015). However, there has been no report on the involvement of *Tlr7* and *Tlr8* in the male reproductive system. Therefore, these genes should be further examined as candidate molecules that might be instrumental in connecting autoimmunity and the male reproductive function.

In conclusion, our results highlight the effect of systemic autoimmune disease on spermatogenesis, characterized with decreased testis weight, increased numbers of residual bodies, and apoptotic germ cells, particularly in St. XII seminiferous tubules without typical inflammation. In addition, we provide evidence for the possible effect of an autoimmunity condition on Sertoli cells, which can subsequently cause the failure of spermatogenesis. Further investigation of the mechanism of testicular phenotypes in BXS<sup>B</sup>-*Yaa* would reveal pathogenesis of spermatogenesis disorder accompanying systemic autoimmune disease.

## **Compliance with Ethical Statements**

### **Conflict of Interest**

The authors have no conflicts of interest directly relevant to the content of this article.

### **Funding**

This study was supported in part by JSPS KAKENHI (grant number JP18J22455) (Ms. Otani).

### **Ethical approval**

All animal experiments were approved by the Institutional Animal Care and Use Committee, Hokkaido University and the Faculty of Veterinary Medicine, Hokkaido University (approval No. 15-0079, 16-0124; approved by the Association for Assessment and Accreditation of Laboratory Animal Care International).



## References

- Andrews BS, Eisenberg RA, Theofilopoulos AN, et al (1978) Spontaneous murine lupus-like syndromes. Clinical and immunopathological manifestations in several strains. *J Exp Med* 148:1198–215. doi: 10.1084/jem.148.5.1198
- Boehm GW, Sherman GF, Hoplight BJ, et al (1998) Learning in Year-Old Female Autoimmune BXSB Mice. *Physiol Behav* 64:75–82. doi: 10.1016/S0031-9384(98)00027-4
- Borg CL, Wolski KM, Gibbs GM, O'Bryan MK (2010) Phenotyping male infertility in the mouse: how to get the most out of a “non-performer”. *Hum Reprod Update* 16:205–24. doi: 10.1093/humupd/dmp032
- Creasy D, Bube A, de Rijk E, et al (2012) Proliferative and nonproliferative lesions of the rat and mouse male reproductive system. *Toxicol. Pathol.* 40
- Cui D, Han G, Shang Y, et al (2015) Antisperm antibodies in infertile men and their effect on semen parameters: A systematic review and meta-analysis. *Clin Chim Acta* 444:29–36. doi: 10.1016/j.cca.2015.01.033
- Fijak M, Meinhardt A (2006) The testis in immune privilege. *Immunol Rev* 213:66–81. doi: 10.1111/j.1600-065X.2006.00438.x
- Firlit CF, Davis JR (1965) Morphogenesis of the residual body of the mouse testis. *J Cell Sci* s3-106: 93-98.
- Fish EN (2008) The X-files in immunity: sex-based differences predispose immune responses. *Nat Rev Immunol* 8:737–744. doi: 10.1038/nri2394
- Garcia PC, Rubio EM, Pereira OCM (2007) Antisperm antibodies in infertile men and their correlation with seminal parameters. *Reprod Med Biol* 6:33–38. doi: 10.1111/j.1447-0578.2007.00162.x
- Giampietri C, Petrungaro S, Coluccia P, et al (2005) Germ cell apoptosis control during

493 spermatogenesis. *Contraception* 72:298–302. doi:  
 494 10.1016/J.CONTRACEPTION.2005.04.011

495 Goswami D, Conway GS (2007) Premature ovarian failure. *Horm Res* 68:196–202. doi:  
 496 10.1159/000102537

497 Hess RA (2002) The Efferent Ductules: Structure and Functions. In: *The Epididymis: From*  
 498 *Molecules to Clinical Practice*. Springer US, pp 49–80

499 Hu J, Song D, Luo G, et al (2015) Activation of Toll like receptor 3 induces spermatogonial  
 500 stem cell apoptosis. *Cell Biochem Funct* 33:415–422. doi: 10.1002/cbf.3133

501 Jiang X, Ma T, Zhang Y, et al (2015) Specific Deletion of Cdh2 in Sertoli Cells Leads to  
 502 Altered Meiotic Progression and Subfertility of Mice1. *Biol Reprod* 92:. doi:  
 503 10.1095/biolreprod.114.126334

504 Kimura J, Ichii O, Nakamura T, et al (2014) BXSb-type genome causes murine autoimmune  
 505 glomerulonephritis: Pathological correlation between telomeric region of chromosome 1  
 506 and Yaa. *Genes Immun* 15:182–189. doi: 10.1038/gene.2014.4

507 Kohno S, Munoz JA, Williams TM, et al (1983) Immunopathology of murine experimental  
 508 allergic orchitis. *J Immunol* 130:2675–82

509 Komatsu K, Manabe N, Kiso M, et al (2003) Changes in localization of immune cells and  
 510 cytokines in corpora lutea during luteolysis in murine ovaries. *J Exp Zool* 296A:152–159.  
 511 doi: 10.1002/jez.a.10246

512 Kon Y, Horikoshi H, Endoh D (1999) Metaphase-specific cell death in meiotic spermatocytes in  
 513 mice. *Cell Tissue Res* 296:359–369. doi: 10.1007/s004410051296

514 Kovats S (2015) Estrogen receptors regulate innate immune cells and signaling pathways. *Cell*  
 515 *Immunol* 294:63–69. doi: 10.1016/j.cellimm.2015.01.018

516 Liu Z, Zhao S, Chen Q, et al (2015) Roles of Toll-Like Receptors 2 and 4 in Mediating

517 Experimental Autoimmune Orchitis Induction in Mice1. Biol Reprod 92:. doi:  
518 10.1095/biolreprod.114.123901

519 Lue Y, Sinha Hikim AP, Wang C, et al (2003) Functional Role of Inducible Nitric Oxide  
520 Synthase in the Induction of Male Germ Cell Apoptosis, Regulation of Sperm Number,  
521 and Determination of Testes Size: Evidence from Null Mutant Mice. Endocrinology  
522 144:3092–3100. doi: 10.1210/en.2002-0142

523 Meistrich ML, Hess RA (2013) Assessment of spermatogenesis through staging of seminiferous  
524 tubules. Methods Mol Biol 927:299–307. doi: 10.1007/978-1-62703-038-0\_27

525 Murphy ED, Roths JB (1979) A y chromosome associated factor in strain bxsB producing  
526 accelerated autoimmunity and lymphoproliferation. Arthritis Rheum 22:1188–1194. doi:  
527 10.1002/art.1780221105

528 Naito M, Terayama H, Hirai S, et al (2012) Experimental autoimmune orchitis as a model of  
529 immunological male infertility. Award Rev Med Mol Morphol 45:185–189. doi:  
530 10.1007/s00795-012-0587-2

531 Otsuka S, Namiki Y, Ichii O, et al (2010) Analysis of factors decreasing testis weight in MRL  
532 mice. Mamm Genome 21:153–161. doi: 10.1007/s00335-010-9251-0

533 Pisitkun P, Deane JA, Difilippantonio MJ, et al (2006) Autoreactive B cell responses to  
534 RNA-related antigens due to TLR7 gene duplication. Science 312:1669–72. doi:  
535 10.1126/science.1124978

536 Saito H, Hara K, Tanemura K (2017) Prenatal and postnatal exposure to low levels of  
537 permethrin exerts reproductive effects in male mice. Reprod Toxicol 74:108–115. doi:  
538 10.1016/J.REPROTOX.2017.08.022

539 Shaha C, Tripathi R, Mishra DP (2010) Male germ cell apoptosis: regulation and biology.  
540 Philos Trans R Soc Lond B Biol Sci 365:1501–15. doi: 10.1098/rstb.2009.0124

541 Silva CA, Cocuzza M, Carvalho JF, Bonfá E (2014) Diagnosis and classification of  
 542 autoimmune orchitis. *Autoimmun Rev* 13:431–434. doi: 10.1016/J.AUTREV.2014.01.024  
 543 Subramanian V V, Hochwagen A (2014) The meiotic checkpoint network: step-by-step through  
 544 meiotic prophase. *Cold Spring Harb Perspect Biol* 6:a016675. doi:  
 545 10.1101/cshperspect.a016675  
 546 Suehiro RM, Borba EF, Bonfa E, et al (2008) Testicular Sertoli cell function in male systemic  
 547 lupus erythematosus. *Rheumatology* 47:1692–1697. doi: 10.1093/rheumatology/ken338  
 548 Suzuka H, Yoshifusa H, Nakamura Y, et al (1993) Morphological analysis of autoimmune  
 549 disease in MRL-lpr,Yaa male mice with rapidly progressive systemic lupus erythematosus.  
 550 *Autoimmunity* 14:275–82  
 551 Terré B, Lewis M, Gil-Gómez G, et al (2019) Defects in efferent duct multiciliogenesis underlie  
 552 male infertility in GEMC1-, MCIDAS- or CCNO-deficient mice. *Dev* 146:. doi:  
 553 10.1242/dev.162628  
 554 Theas MS (2018) Germ cell apoptosis and survival in testicular inflammation. *Andrologia*  
 555 50:e13083. doi: 10.1111/and.13083  
 556 Thomas B, Rutman A, Hirst RA, et al (2010) Ciliary dysfunction and ultrastructural  
 557 abnormalities are features of severe asthma. *J Allergy Clin Immunol* 126:. doi:  
 558 10.1016/j.jaci.2010.05.046  
 559 Trigenaite A, Dimo J, Jørgensen TN (2015) Suppressive effects of androgens on the immune  
 560 system. *Cell Immunol* 294:87–94. doi: 10.1016/j.cellimm.2015.02.004  
 561 Tung KSK, Harakal J, Qiao H, et al (2017) Egress of sperm autoantigen from seminiferous  
 562 tubules maintains systemic tolerance. *J Clin Invest* 127:1046–1060. doi:  
 563 10.1172/JCI89927  
 564 Ullrich S, Gustke H, Lamprecht P, et al (2009) Severe impaired respiratory ciliary function in

565 Wegener granulomatosis. *Ann Rheum Dis* 68:1067–1071. doi: 10.1136/ard.2008.096974  
 566 Wu H, Wang H, Xiong W, et al (2008) Expression Patterns and Functions of Toll-Like  
 567 Receptors in Mouse Sertoli Cells. *Endocrinology* 149:4402–4412. doi:  
 568 10.1210/en.2007-1776  
 569 Xiao C-Y, Wang Y-Q, Li J-H, et al (2017) Transformation, migration and outcome of residual  
 570 bodies in the seminiferous tubules of the rat testis. *Andrologia* 49:e12786. doi:  
 571 10.1111/and.12786  
 572 Yang F, Gell K, van der Heijden GW, et al (2008) Meiotic failure in male mice lacking an  
 573 X-linked factor. *Genes Dev* 22:682–91. doi: 10.1101/gad.1613608  
 574 Yuan S, Liu Y, Peng H, et al (2019) Motile cilia of the male reproductive system require  
 575 miR-34/miR-449 for development and function to generate luminal turbulence. *Proc Natl*  
 576 *Acad Sci U S A* 116:3584–3593. doi: 10.1073/pnas.1817018116  
 577 Zheng K, Yang F, Wang PJ (2010) Regulation of Male Fertility by X-Linked Genes. *J Androl*  
 578 31:79–85. doi: 10.2164/jandrol.109.008193  
 579  
 580  
 581

582

<b>Table 1. Antibodies</b>				
Antibody	Source	Dilution	Antigen retrieval	Treatment
Rabbit anti-CD3	Nichirei (Tokyo, Japan)	1:200	10 mM CB (pH 6.0)	110°C, 15 min
Rat anti-B220	Cedarlane (Ontario, Canada)	1:1600	10 mM CB (pH 6.0)	110°C, 15 min
Rabbit anti-Iba1	Wako (Osaka, Japan)	1:1200	10 mM CB (pH 6.0)	110°C, 15 min
Rabbit anti-ssDNA	IBL (Gunma, Japan)	1:400	-	-
CB: citrate buffer. ssDNA: single-stranded DNA.				

583

584

**Table 2. Primers**

Gene name (accession no.)	Official symbol	Primer sequence (5'-3')	Primer position (5'-3') (bp)	Product size (bp)
Actin, beta (NM_007393)	<i>Actb</i>	F: TGTTACCAACTGGGACGACA R: GGGGTGTTGAAGGTCTCAA	334-353 498-479	165
Interleukin 1 alpha (NM_010554)	<i>Il1a</i>	F: AGATGACCTGCAGTCCATAACC R: GACAAACTTCTGCCTGACGAG	351-372 471-451	121
Nitric oxide synthase 2, inducible (NM_010927)	<i>Nos2</i>	F: AGCTGATGGTCAAGATCCAGAG R: GTGCATACCACTTCAACCCGA	1167-1188 1282-1262	116
Interleukin 1 beta (NM_008361)	<i>Il1b</i>	F: TTCCAGGATGAGGACATGAGC R: AATGGGAACGTCACACACCAG	337-357 447-427	111
Tumor necrosis factor (NM_013693)	<i>Tnf</i>	F: TCTTCTCATTCTGCTTGTGGC R: CATAGAACTGATGAGAGGGAGGC	271-292 389-367	119
Interleukin 6 (NM_031168)	<i>Il6</i>	F: CAACGATGATGCACTTGCAGA R: GGTACTCCAGAAGACCAGAGGA	312-332 439-418	128
Interleukin 10 (NM_010548)	<i>Il10</i>	F: GCATTTGAATTCCCTGGGTGAG R: TTGTAGACACCTTGGTCTTGGAG	388-409 534-512	147
Transforming growth factor, beta 1 (NM_011577)	<i>Tgfb1</i>	F: ATGCTAAAGAGGTCACCCGC R: TGCTTCCCGAATGTCTGACG	1178-1197 1296-1277	119

586

587

**Table 3. Correlation of autoimmune indices with examined parameters of the mouse testes**

Parameter			T/B	Number of residual bodies in total	Number of ssDNA-positive cells in total	Number of Sertoli cells in total
			All / BXSB- <i>Yaa</i>	All / BXSB- <i>Yaa</i>	All / BXSB- <i>Yaa</i>	All / BXSB- <i>Yaa</i>
12-week-old	S/B	$\rho$	-.357 / -.400	.414 / .900*	.711** / -.700	-.443 / .500
		$P$	.191 / .505	.125 / .037	.003 / .188	.098 / .391
	Anti-dsDNA antibody	$\rho$	-.071 / .000	.767** / .800	.295 / -.600	-.600* / .300
		$P$	.800 / 1.000	.001 / .104	.286 / .285	.018 / .624
24-week-old	S/B	$\rho$	.111 / -.800	.489 / .100	.650** / -.500	.221 / .100
		$P$	.694 / .104	.064 / .873	.009 / .391	.428 / .873
	Anti-dsDNA antibody	$\rho$	.011 / -.500	.446 / -.200	.575* / .100	.321 / .700
		$P$	.970 / .391	.095 / .747	.025 / .873	.243 / .188
12- and 24-week-old	S/B	$\rho$	-.127 / -.758*	.296 / .200	.713** / -.539	-.057 / .552
		$P$	.504 / .011	.112 / .580	.000 / .108	.766 / .098
	Anti-dsDNA antibody	$\rho$	-.177 / -.345	.621** / .212	.400* / -.273	-.155 / .406
		$P$	.350 / .328	.000 / .556	.028 / .446	.414 / .244

\* $P < 0.05$ , \*\*  $P < 0.01$ .  $\rho$ : Spearman's rank correlation coefficient, N = 14-30 (all strains), 5-10 (BXSB-*Yaa*). All: C57BL/6N, BXSB, and BXSB-*Yaa*. T/B: ratio of testis weight to body weight; S/B: ratio of spleen weight to body weight; dsDNA: double-stranded DNA.



588 **Table 4. Correlation of autoimmune indices with examined parameters of the mouse testes**

Parameter			Number of	Number of	Number of	Number of	Number of	Number of
			residual bodies at	ssDNA-positive	ssDNA-positive	Sertoli cells at St.	Sertoli cells at St.	Sertoli cells at St.
			St. VIII	cells at St. IV	cells at St. XII	IV	V	IX
			All / BXSB- <i>Yaa</i>	All / BXSB- <i>Yaa</i>	All / BXSB- <i>Yaa</i>	All / BXSB- <i>Yaa</i>	All / BXSB- <i>Yaa</i>	All / BXSB- <i>Yaa</i>
12-week-old	S/B	$\rho$	.157 / -.300	.487 / .300	.470 / .900*	-.736** / .100	-.600* / .900*	.467 / .800
		$P$	.576 / .624	.065 / .624	.077 / .037	.002 / .873	.018 / .037	.079 / .104
	Anti-dsDNA antibody	$\rho$	.597* / -.100	.030 / .100	.567* / 1.000**	-.522* / .200	-.636* / .700	-.386 / .000
		$P$	.019 / .873	.914 / .873	.027 / .000	.046 / .747	.011 / .188	.155 / 1.000
24-week-old	S/B	$\rho$	.371 / .354	-.338 / .894*	.657** / -.100	.175 / .200	-.011 / -.100	.417 / -.300
		$P$	.173 / .559	.219 / .041	.008 / .873	.533 / .747	.970 / .873	.122 / .624
	Anti-dsDNA antibody	$\rho$	.482 / -.200	-.433 / -.112	.739** / .200	.236 / .200	.204 / .700	.411 / .000
		$P$	.069 / .747	.107 / .858	.002 / .747	.398 / .747	.467 / .188	.128 / 1.000
12- and 24-week-old	S/B	$\rho$	.290 / .406	.062 / -.485	.543** / .442	-.239 / .406	-.253 / .539	.392* / .333
		$P$	.121 / .244	.745 / .156	.002 / .200	.204 / .244	.178 / .108	.032 / .347
	Anti-dsDNA antibody	$\rho$	.567** / .042	-.249 / -.301	.624** / .527	-.174 / .333	-.255 / .564	.049 / .188
		$P$	.001 / .907	.185 / .339	.000 / .117	.359 / .347	.173 / .090	.795 / .603

\* $P < 0.05$ , \*\*  $P < 0.01$ .  $\rho$ : Spearman's rank correlation coefficient, N = 14-30 (all strains), 5-10 (BXSB-*Yaa*). All: C57BL/6N, BXSB, and BXSB-*Yaa*. T/B: ratio of testis weight to body weight; S/B: ratio of spleen weight to body weight; dsDNA: double-stranded DNA.

## Figure Legends

### **Figure 1. Indices of autoimmune disease condition and male reproductive function in mice**

(a) Bodyweight. (b) The ratio of spleen weight to body weight. (c) The concentration of anti-dsDNA antibody in the serum. (d) Testis weight. (e) The ratio of testis weight to body weight. Each bar represents mean  $\pm$  SE ( $n \geq 5$ ). Significant differences among strains are shown by the letters above each bar. A lowercase letter represents the difference in 12-week-old mice. An uppercase letter represents the difference in 24-week-old mice.  $P < 0.05$  (Scheffe's method). Significant differences between different ages in the same strain are indicated with an asterisk. \*:  $P < 0.05$ , \*\*:  $P < 0.01$  (Mann-Whitney  $U$ -test). (f) Correlation between the ratio of testis weight to body weight and that of spleen in BXSB-*Yaa*.  $\rho$ : Spearman's rank correlation coefficient ( $n = 26$ ).  $P = 0.001$ .

### **Figure 2. Comparison of histopathological features in mouse testes and epididymis**

(a-f) Representative images of the testes and epididymides of C57BL/6N (a and d), BXSB (b and e), and BXSB-*Yaa* (c and f) at 12 weeks of age. Bidirectional arrows represent the lumen of the seminiferous tubules. Asterisks (\*) represent the loss of sperm in the lumen of the tail of the epididymis. (g-h) Representative images of histopathology in BXSB-*Yaa* testis at 24 weeks (g) and 12 weeks (h) of age. Arrowheads represent multinucleated cells. The asterisk shows the rete

testis dilated and filled with sperm. RT: rete testis. (i-k) Histology of St. VIII seminiferous tubules of 12-week-old C57BL/6N (i), BXSB (j), and BXSB-*Yaa* (k). Arrowheads represent residual bodies. (l-m) The number of residual bodies per unit area of total (l) and St. VIII seminiferous tubules (m). Each bar represents mean  $\pm$  SE (n = 5). Significant differences among strains are shown by the letters above each bar.  $P < 0.05$  (Scheffe's method). A lowercase letter represents the difference in 12-week-old mice. An uppercase letter represents the difference in 24-week-old mice. Significant differences between different ages in the same strain are indicated with an asterisk. \*:  $P < 0.05$  (Mann-Whitney *U*-test). (n) Representative image of an atypical residual body in St. XII seminiferous tubules of 12-week-old BXSB-*Yaa*. All sections were fixed with Bouin's fluid and stained with PAS-hematoxylin. Roman numerals indicate the stage of the seminiferous epithelial cycle.

### **Figure 3. Analysis of the immunological changes in mouse testes**

(a-i) Immunostained sections of mouse testes fixed with 4% paraformaldehyde. Immunohistochemistry for CD3 (a-c), B220 (d-f), and Iba1 (g-i) in cross seminiferous tubules in C57BL/6N, BXSB, and BXSB-*Yaa* at 12 weeks of age. Arrowheads represent macrophages. Sections of the spleen are shown in insets. Bars = 100  $\mu$ m. Bars (insets) = 10  $\mu$ m.

(j) Relative mRNA expression of inflammation-related genes in C57BL/6N, BXSB, and

BXSB-*Yaa* testes. The expression levels were normalized to the levels of *Actb*. Each bar represents mean  $\pm$  SE (n = 5).

**Figure 4. Analysis of apoptotic cells in mouse testes**

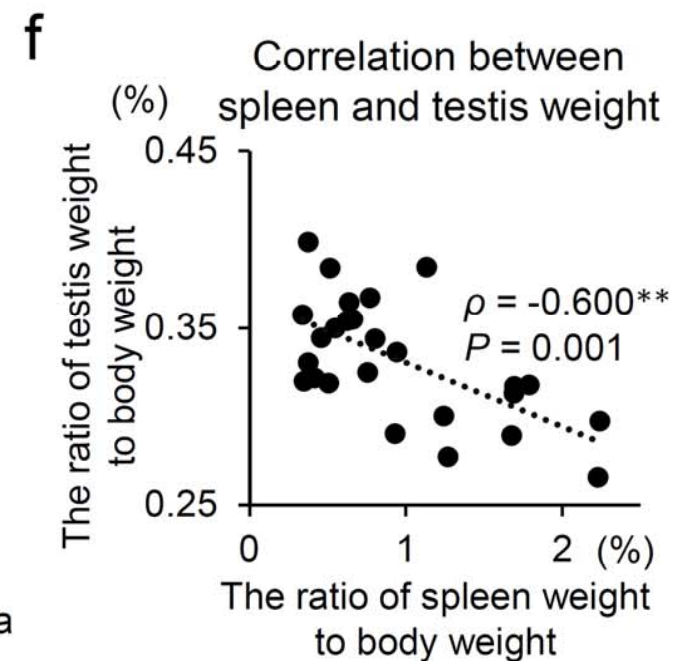
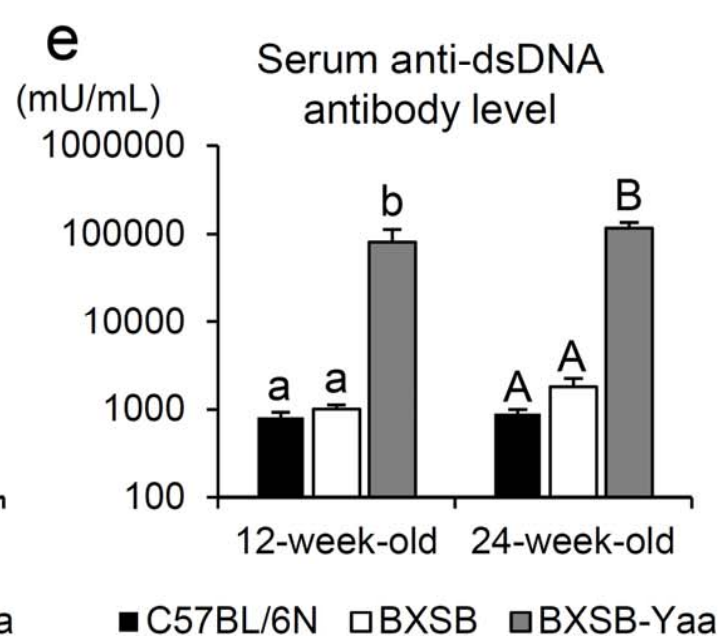
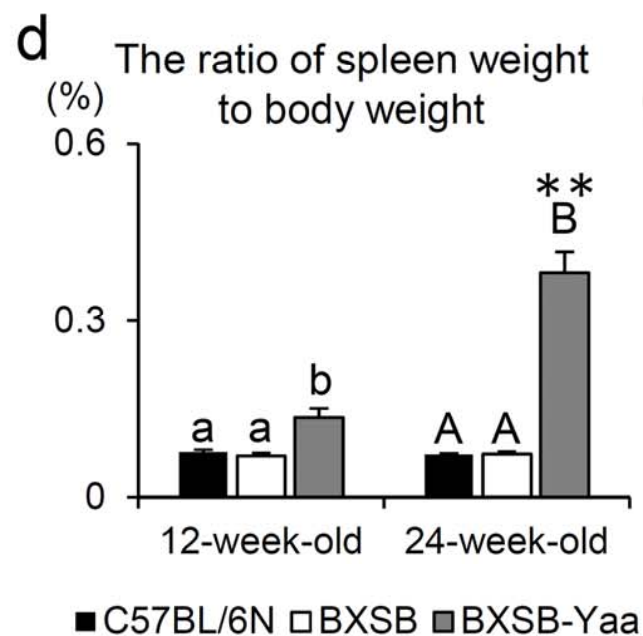
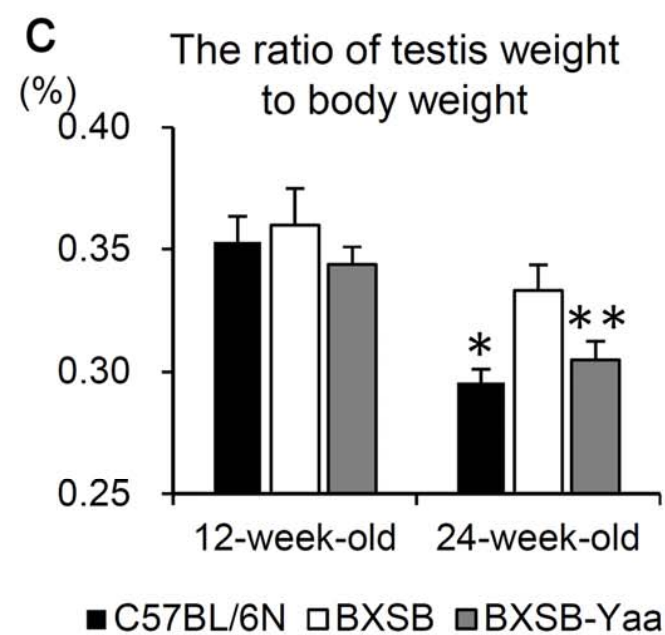
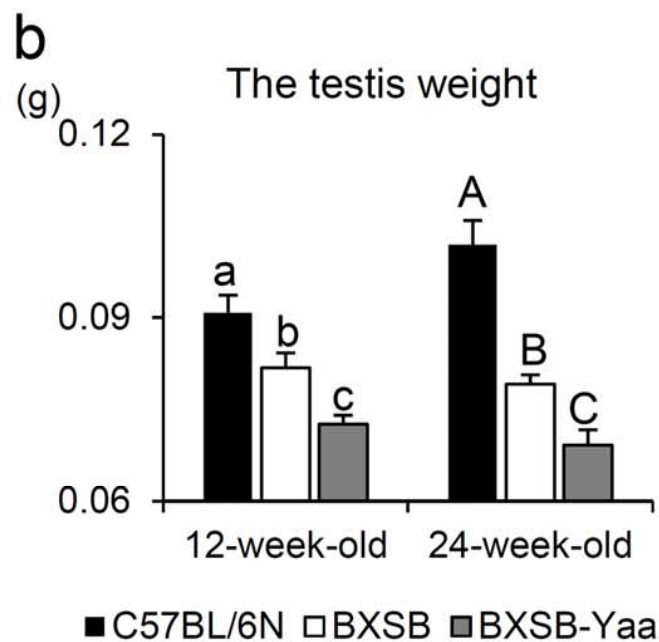
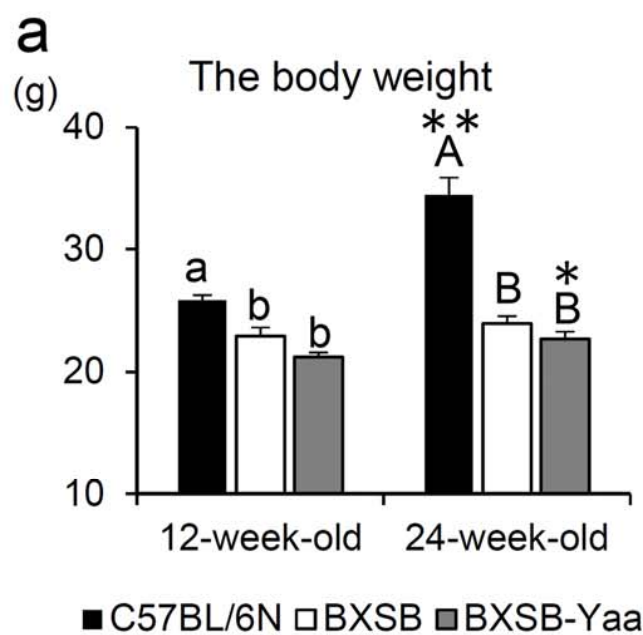
(a-c) Immunostaining of ssDNA in cross seminiferous tubules at St. XII in 12-week-old C57BL/6N (a), BXSB (b), and BXSB-*Yaa* (c). Arrowheads represent apoptotic cells. Bars = 50  $\mu$ m.

(d-e) The number of ssDNA-positive cells per unit area of all examined (d) and each stage (e) seminiferous tubules in a section of mouse testis. Each bar represents mean  $\pm$  SE (n = 5). Roman numerals indicate the stage of the seminiferous epithelial cycle. Significant differences among strains are shown by the letters above each bar.  $P < 0.05$  (Scheffe's method). A lowercase letter represents the difference in 12-week-old mice. An uppercase letter represents the difference in 24-week-old mice. Significant differences between different ages in the same strain are indicated with an asterisk. \*:  $P < 0.05$ , \*\*:  $P < 0.01$  (Mann-Whitney *U*-test).

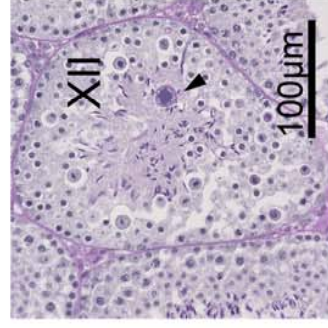
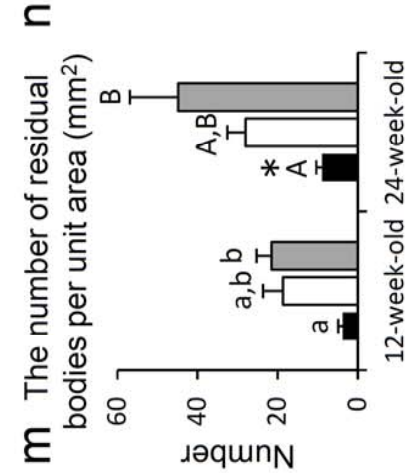
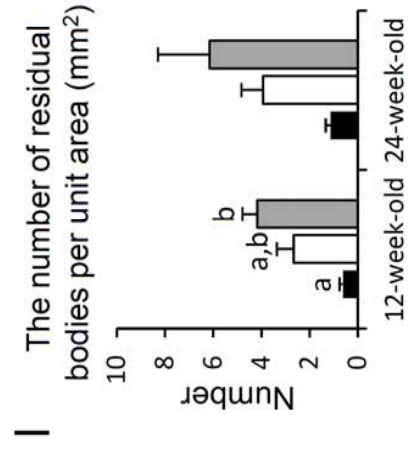
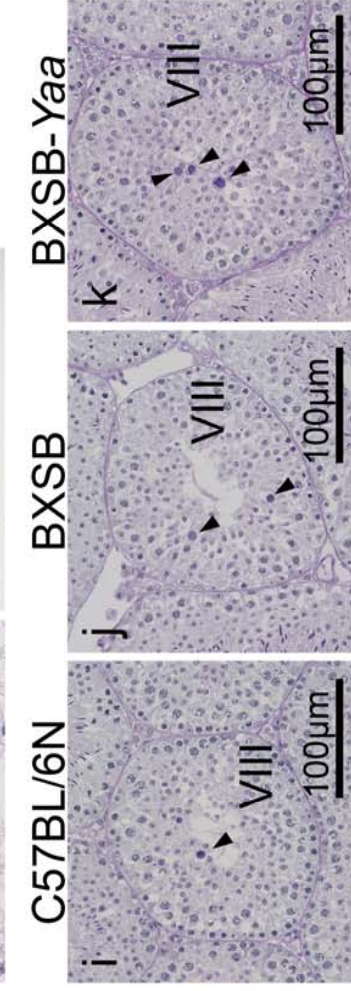
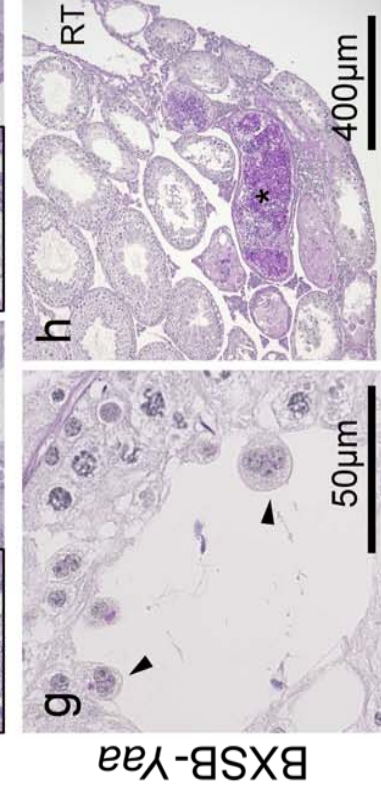
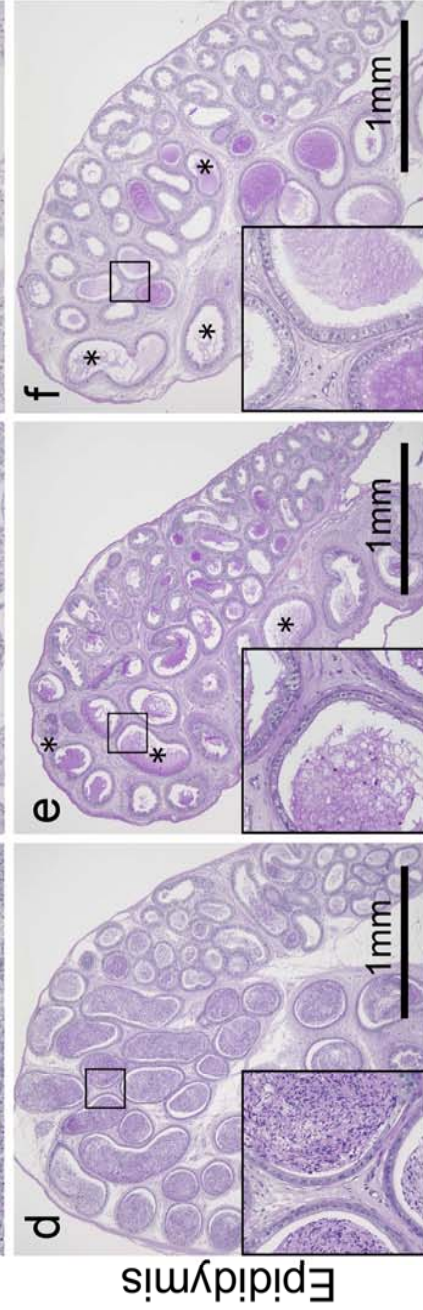
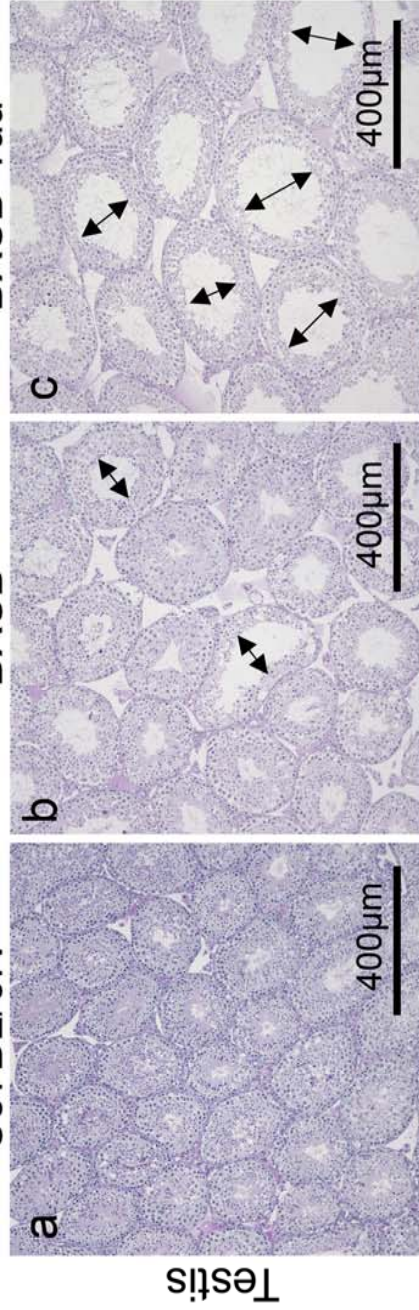
(f-h) Histology of Sertoli cells in cross seminiferous tubules at St. IV-V in 12-week-old C57BL/6N (f), BXSB (g), and BXSB-*Yaa* (h). Sections were fixed with Bouin's fluid and stained with PAS-hematoxylin. Arrowheads represent Sertoli cells. Bars = 20  $\mu$ m.

(i-j) The number of Sertoli cells per unit area of total (i) and each stage (j) seminiferous tubules

643 in a section of mouse testis. Each bar represents mean  $\pm$  SE (n = 5). Roman numerals indicate  
644 the stage of the seminiferous epithelial cycle. Significant differences among strains are indicated  
645 with letters above each bar.  $P < 0.05$  (Scheffe's method). A lowercase letter represents the  
646 difference in 12-week-old mice. Significant differences between different ages in the same  
647 strain are indicated with an asterisk. \*:  $P < 0.05$ , \*\*:  $P < 0.01$  (Mann-Whitney *U*-test).  
648





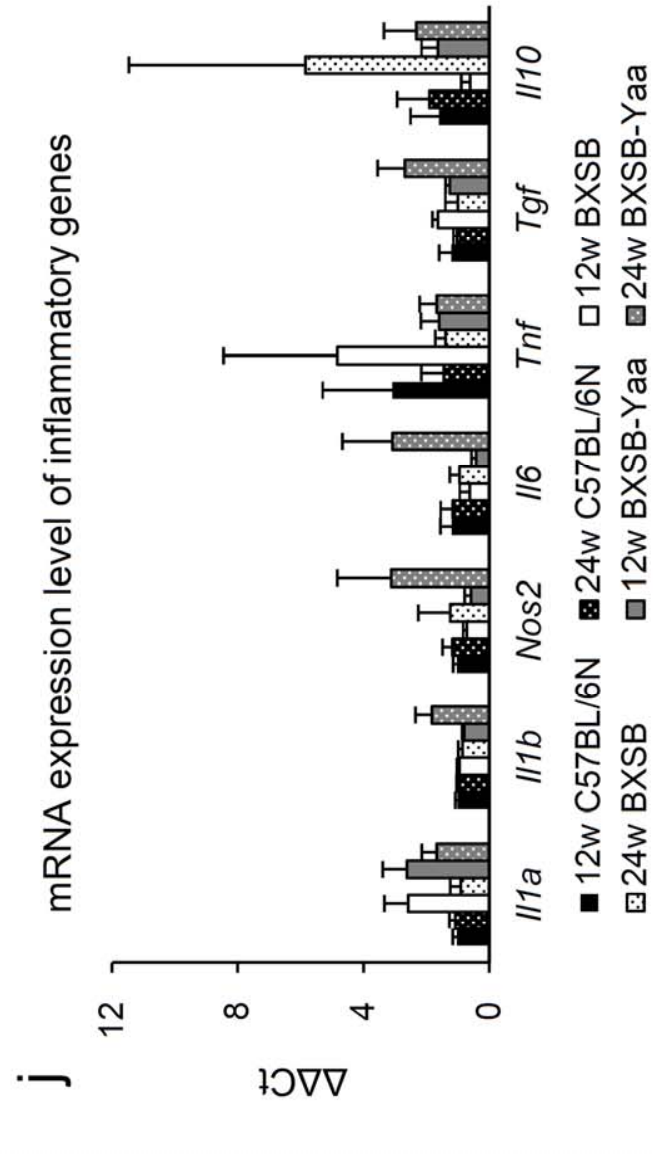
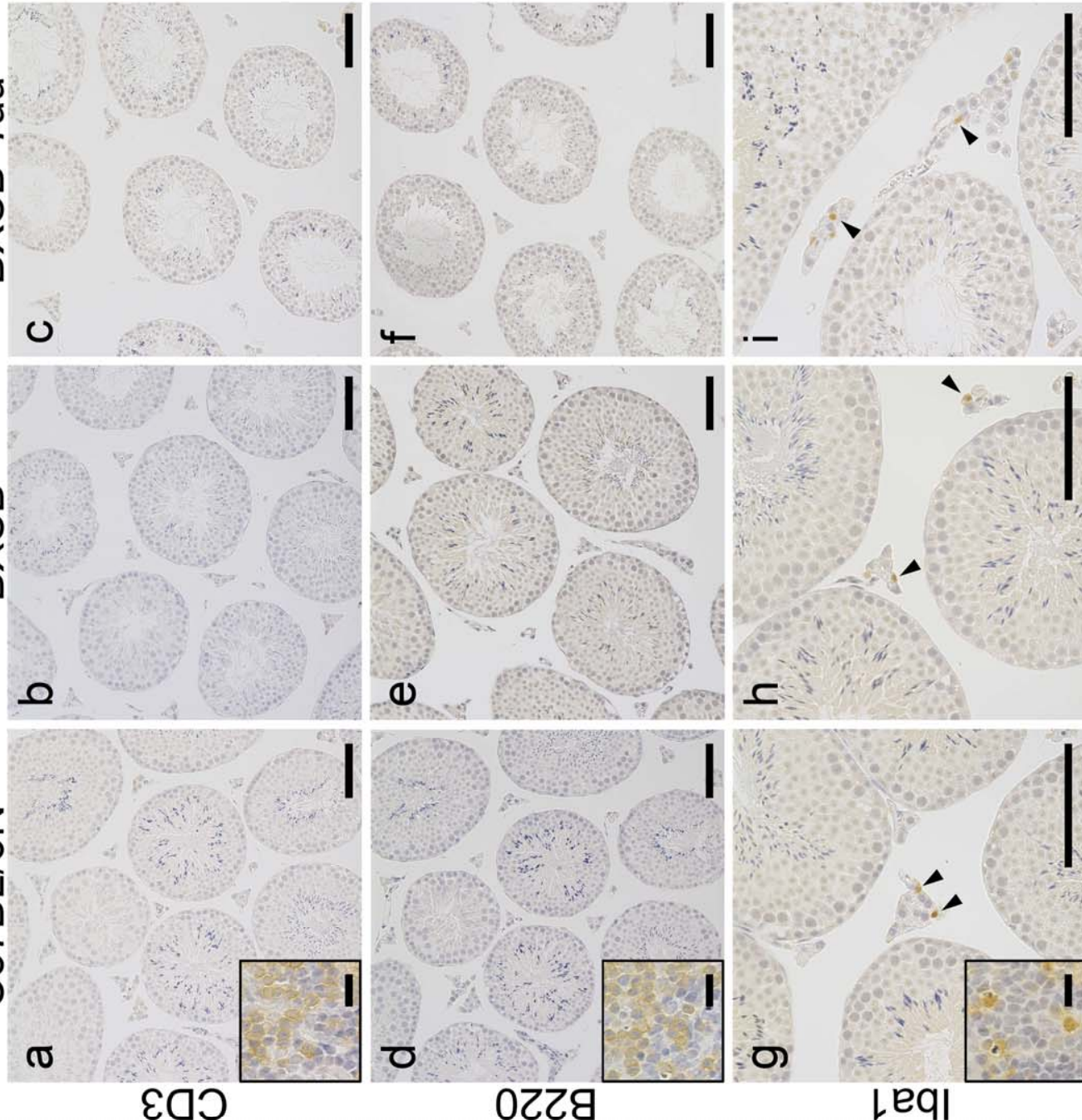




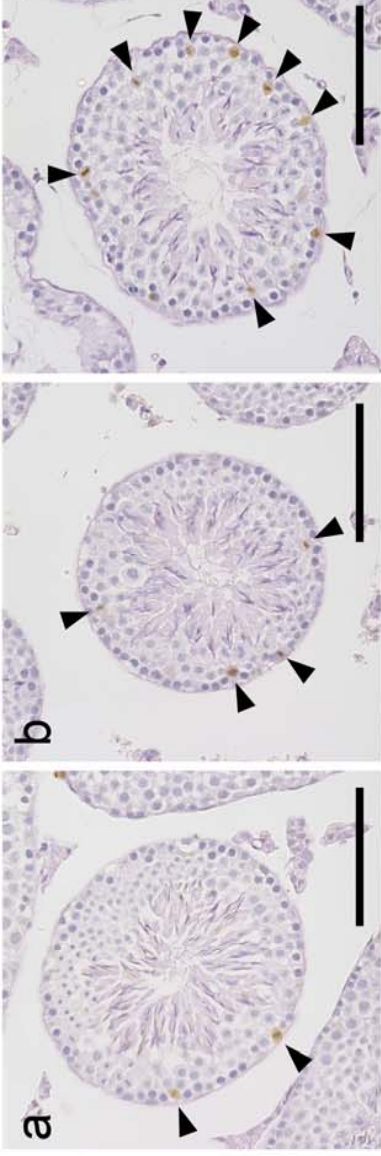
C57BL/6N

BXSB

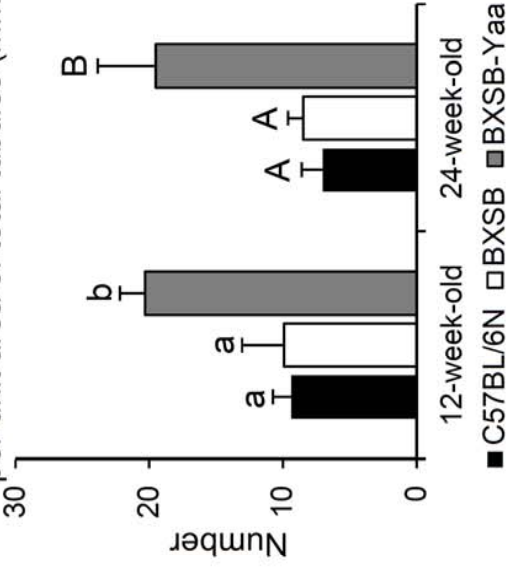
BXSB-Yaa



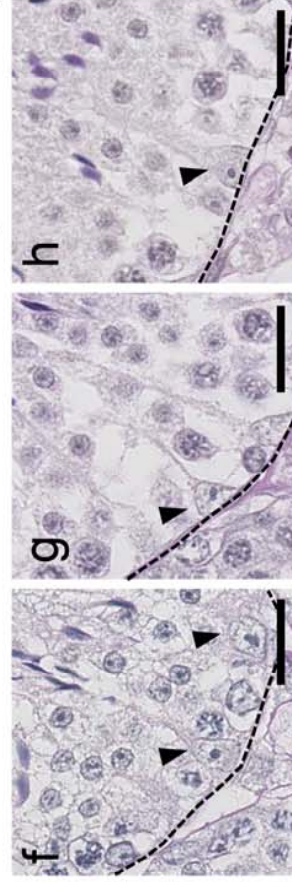
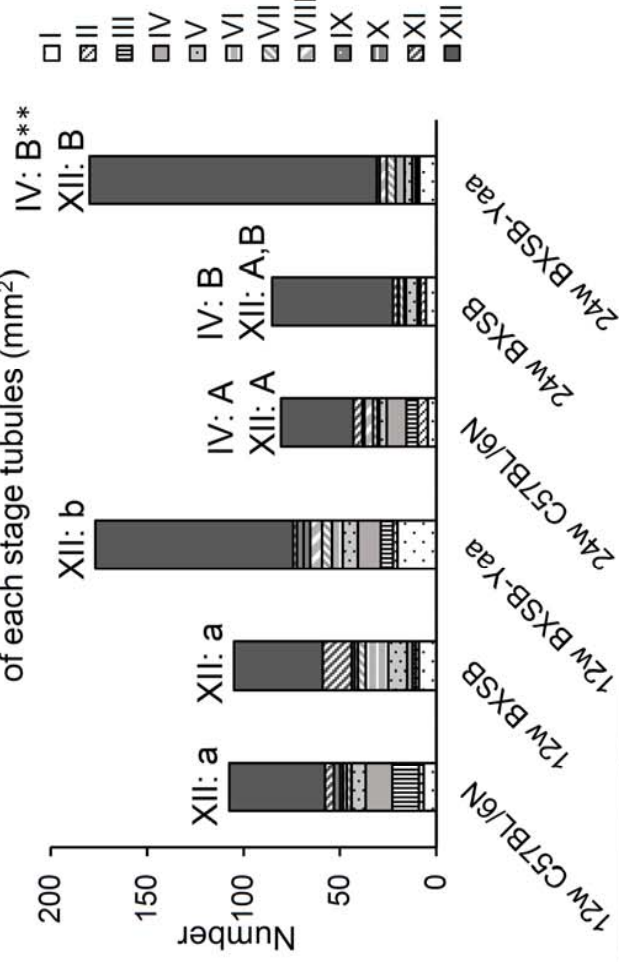




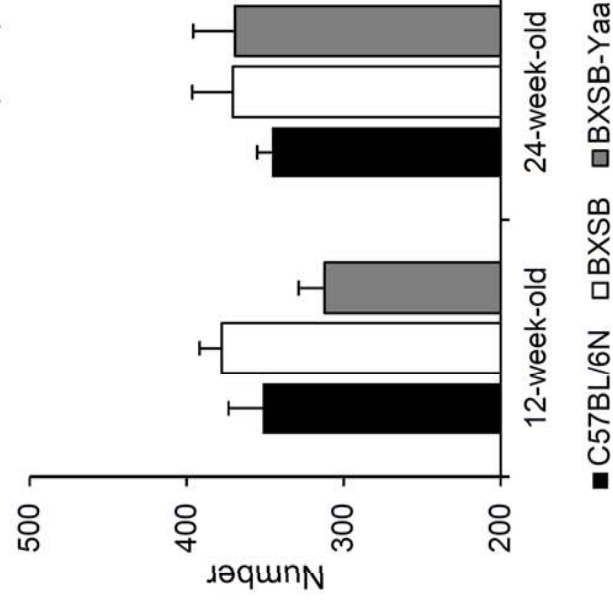
**d** The number of ssDNA-positive cells per unit area of total tubules ( $\text{mm}^2$ )



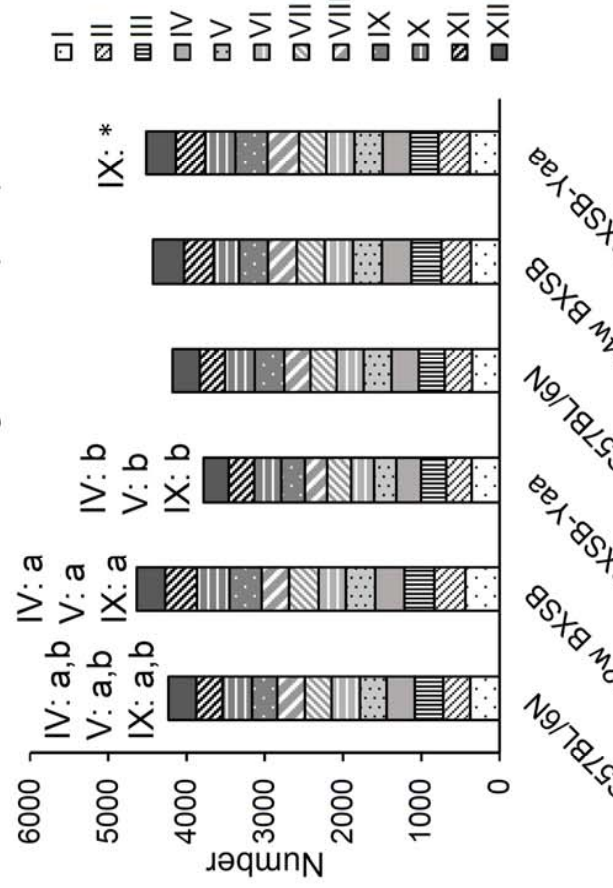
**e** The number of ssDNA-positive cells per unit area of each stage tubules ( $\text{mm}^2$ )



**i** The number of Sertoli cells per unit area of total tubules ( $\text{mm}^2$ )



**j** The number of Sertoli cells per unit area of each stage tubules ( $\text{mm}^2$ )



**Supplemental Table 1. Correlation of autoimmune indices with examined parameters in all mice**

Parameter			Number of residual bodies	Number of ssDNA-positive cells	Number of Sertoli cells
12-week-old	S/B	$\rho$	-	I 0.624*; VIII 0.640*	IV -0.757**; V -0.600*
	Anti-dsDNA antibody	$\rho$	VIII 0.597*; IX 0.625*	XII 0.567*	IV -0.522*; V -0.636*; VI; -0.665**; VIII -0.617*
24-week-old	S/B	$\rho$	III 0.592*; VIII 0.579*	VI 0.524*; X -0.608*; XII 0.650**	-
	Anti-dsDNA antibody	$\rho$	-	XI -0.603*, XII 0.739**	-
12- and 24-week-old	S/B	$\rho$	III 0.433*; IX 0.392*	I 0.387*; VI 0.454*; XI -0.370*; XII 0.543**	-
	Anti-dsDNA antibody	$\rho$	VIII 0.567**; IX 0.563**; X 0.430*	XI -0.417*, XII 0.624**	-

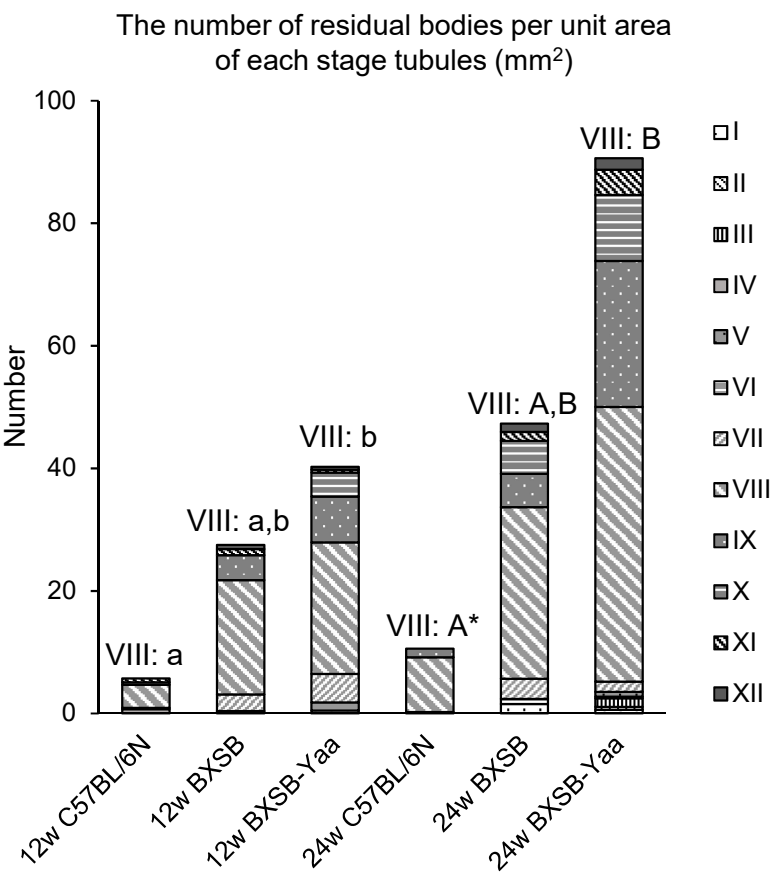
\* $P < 0.05$ , \*\*  $P < 0.01$ .  $\rho$ : Spearman's rank correlation coefficient, N = 15-30. All: C57BL/6N, BXSB, and BXSB-*Yaa*. S/B: ratio of spleen weight to body weight; dsDNA: double-stranded DNA.

**Supplemental Table 2. Correlation of autoimmune indices with examined parameters in BXSB-*Yaa* mice**

Parameter			Number of residual bodies	Number of ssDNA-positive cells	Number of Sertoli cells
12-week-old	S/B	$\rho$	VI 0.900*; VII 0.975**	XI 0.895*; XII 0.900*	V 0.900*
	Anti-dsDNA antibody	$\rho$	IX 0.900*	XII 1.000**	-
24-week-old	S/B	$\rho$	-	-	-
	Anti-dsDNA antibody	$\rho$	-	VI 0.900*	-
12- and 24-week-old	S/B	$\rho$	III 0.701*	III -0.725*	VIII 0.661*
	Anti-dsDNA antibody	$\rho$	-	-	VII 0.697*

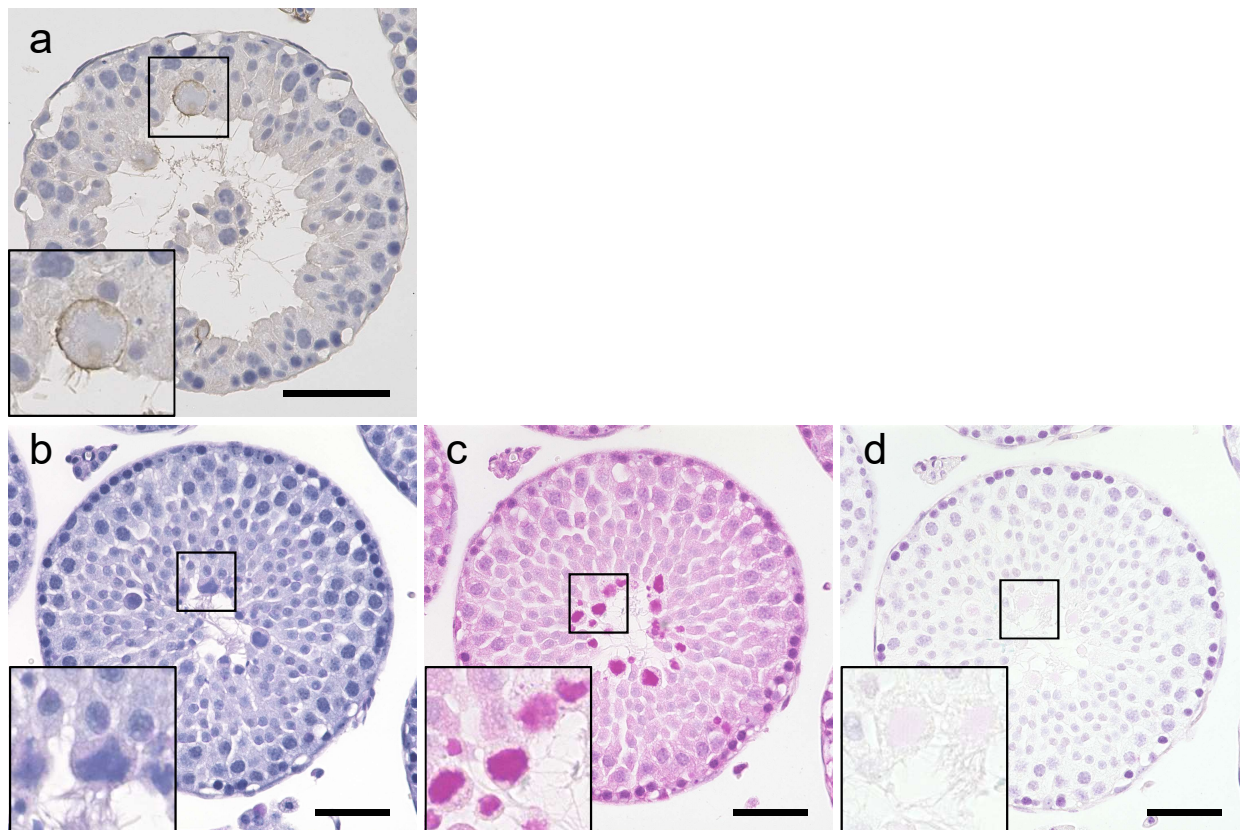
\* $P < 0.05$ , \*\*  $P < 0.01$ .  $\rho$ : Spearman's rank correlation coefficient, N = 5-10 (BXSB-*Yaa*). S/B: ratio of spleen weight to body weight; dsDNA: double-stranded DNA.

# Supplemental Figure 1



Supplemental Figure 1. The number of residual bodies per unit area of each St. seminiferous tubules. Each bar represents mean  $\pm$  SE (n = 5). Significant differences among strains are shown by the letters above each bar.  $P < 0.05$  (Scheffe's method). A lowercase letter represents the difference in 12-week-old mice. An uppercase letter represents the difference in 24-week-old mice. Significant differences between different ages in the same strain are indicated with an asterisk. \*:  $P < 0.05$  (Mann-Whitney  $U$ -test).

## Supplemental Figure 2



Supplemental Figure 2. Morphology of residual bodies in BXSB-*Yaa* seminiferous tubules.

(a) Immunohistochemistry for tACE in cross seminiferous tubules in BXSB-*Yaa* at 12 weeks of age. For antigen retrieval, deparaffinized sections were incubated in buffered citrate (pH 6.0) for 15 min at 110 °C, and then the samples were soaked in methanol containing 0.3% H<sub>2</sub>O<sub>2</sub> to block internal peroxidase activity. After blocked in 10% normal goat serum (SABPO(R) Kit, Nichirei, Tokyo, Japan) for 1 hour at room temperature, sections were incubated with antibody against mouse testicular isoform of angiotensin-converting enzyme (tACE, 1:50, MBL, Nagoya, Japan) at 4 °C overnight. After washing 3 times in phosphate buffered saline, sections were incubated with biotin-conjugated goat anti-mouse IgG antibody (SouthernBiotech, Alabama, USA) for 30 min at room temperature, washed again, and incubated with streptavidin-biotin complex (SABPO(R) Kit, Nichirei) for 30 min. The sections were then incubated with 3, 3'-diaminobenzidine tetrahydrochloride-H<sub>2</sub>O<sub>2</sub> solution. Finally, the sections were counterstained with hematoxylin staining.

(b-d) Representative images of 12-week-old BXSB-*Yaa* seminiferous tubule stained with PAS-hematoxylin (b), methyl green-pyronin (c), and methyl green-pyronin with pre-treatment of RNase (d). To detect accumulated RNA in seminiferous tubules, deparaffinized sections were stained with methyl green-pyronin solution (Nacalai Tesque, Kyoto, Japan) for 10 min at room temperature, then washed with distilled water, and cleared with butanol (c). For further analysis, deparaffinized sections were treated with 0.01% RNase A (Nacalai Tesque, Kyoto, Japan) for 20 minutes at 37 °C before stained with methyl green-pyronin to confirm the existence of RNA (d). Bars = 50 μm. All sections were fixed in 4% paraformaldehyde.